11.1 THE LONG-TERM EVOLUTION OF OZONE AND TEMPERATURE IN THE UPPER STRATOSPHERE

Wolfgang Steinbrecht *, Hans Claude, and Fritz Schönenborn
Deutscher Wetterdienst, Hohenpeissenberg, Germany

ABSTRACT

Space- and ground-based measurements near five stations of the Network for the Detection of Atmospheric Composition Change (NDACC) demonstrate the evolution of upper stratospheric ozone and temperature over the last 30 years. At all stations, ozone has been decreasing by about 15% from 1979 to the late 1990s. Since then, however, ozone levels have been stable or slightly increasing. This evolution is consistent with the strong increase of anthropogenic chlorine from 1979 until the late 1990s, and the beginning chlorine decline achieved by the 1987 Montreal protocol. Agreement between different instruments, as well as with CCMVal model simulations is good. The situation is less clear for upper stratospheric temperature. Measurements at the stations show good agreement with NCEP and ERA-40 analyses, but higher variability than zonal means. Only the wide zonal mean SSU data, which also average over a very wide altitude range, show a clear cooling by about 1 K per decade until around 1995 – in agreement with the CCMVal simulations. This cooling is not clear in most of the other data sets, which show high variability around a more or less stable level since the mid 1990s. Additional temperature data sources and further investigations are needed to determine whether the upper stratospheric is cooling by about -0.8 K per decade, as expected from the continuing increase of CO_2 in the CCMVal simulations.

1. INTRODUCTION

The largest heating and cooling rates in the middle atmosphere occur in the upper stratosphere, near 50 km altitude. 10 K per day are exceeded. At these altitudes, temperatures are fairly high, and emitted radiation can escape to space easily. As indicated in Fig. 1, CO_2 is the main contributor to the cooling. The main heating source is absorption of incoming solar ultra-violet radiation by ozone. Through infrared emissions ozone also contributes to the cooling.

Over the last decades, anthropogenic emissions have changed the atmospheric abundances of both ozone and CO_2. This has affected heating and cooling rates. As shown in Fig. 2, it has resulted in long-term cooling of the upper stratosphere by around -1 K per decade (Ramaswamy et al., 2001; Randel et al. 2009).

* *Corresponding author address:* Wolfgang Steinbrecht, Deutscher Wetterdienst, Met. Obs. Hohenpeissenberg, Albin-Schwaiger-Weg 10, D−82383 Hohenpeissenberg, Germany. e-mail: wolfgang.steinbrecht@dwd.de.

In the past, increasing CO_2 and decreasing ozone, caused by anthropogenic chlorine emissions, have both driven the radiative equilibrium towards colder temperatures. CO_2 is continuing to increase. Chlorine emissions, however, have been curbed by the 1987 Montreal Protocol, and its amendments. Since about 2000, chlorine levels in the stratosphere have started to decrease (WMO, 2007). An end of the ozone decline, and first signs of a beginning increase have

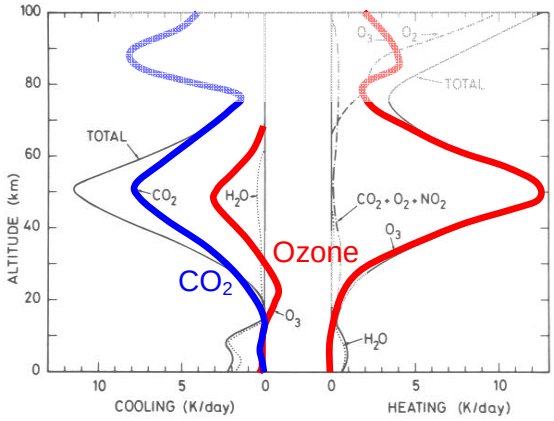

Fig. 1. Typical atmospheric heating and cooling rates as a function of altitude. In the stratosphere, CO2 and ozone are the main contributors to cooling and heating, respectively. After London (1980).

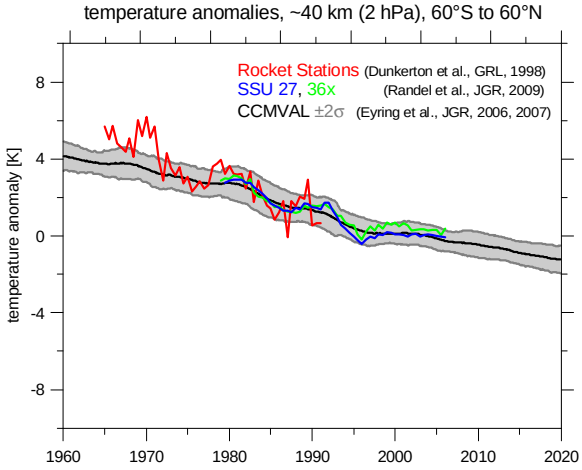

Fig. 2. Evolution of extra-polar (60°S to 60°N) temperature anomalies at about 40 km altitude (2 hPa pressure level), from SSU channel 27 and 36x measurements onboard the NOAA satellites (Randel et al. 2009), and from chemistry climate model simulations by the CCMVAL group (grey underlay, Eyring et al. 2006). The rocket-sonde record compiled by Dunkerton et al. (1998) is plotted as well.

been observed (Newchurch et al., 2003; Steinbrecht et al., 2006). Over the coming decades it will be interesting to see, if and how ozone increase and temperature decline will continue.

In this contribution, we use ground- and space-based records of ozone and temperature, to demonstrate the main long-term variations of both quantities from 1979 to 2009. We compare the observed evolution with results from 3-D chemistry climate model simulations collected under the CCMVal initiative (Eyring et al., 2006).

2. DATA

Our investigation uses ground based ozone and temperature profiles, measured since the late 1980s by lidar at five stations of the Network for the Detection of Atmospheric Composition Change, (NDACC, formerly NDSC, http://www.ndacc.org). The stations are: Hohenpeissenberg (47.8°N; 11.0°E), Observatoire de Haute Provence (43.9°N, 4.4°E), Table Mountain(34.4°N, 117.7°W), Mauna Loa (19.5°N, 155.6°W), and Lauder (45.0°S, 169.7°E). At the Mauna Loa and Lauder sites, as well as at Bern (47.0°N, 7.4°E, close to Hohenpeissenberg and Haute Provence), the lidars are complemented by ground-based microwave radiometers. These have been measuring routine ozone profiles since the early 1990s. All ground-based ozone and temperature profiles were obtained from the NDAAC website (http://www.ndacc.org).

Space based ozone profiles are provided by the Stratospheric Aerosol and Gases Experiments (SAGE I and II, http://eosweb.larc.nasa.gov), and the Halogen Occultation Experiment (HALOE, http://haloe.gats-inc.com). SAGE measured ozone profiles from 1978 to 1980, and from 1984 to 2005. HALOE covered the 1992 to 2005 period, with measurements of both ozone and temperature (in the upper stratosphere). The longest ozone record, from late 1978 until now, however, comes from the series of SBUV instruments. Here we used the MOD-V8 data set assembled at NASA's Goddard Space Flight Center (http://acdb-ext.gsfc.nasa.gov/Data_services/merged/index.html).

Although several other satellite instruments have been measuring ozone profiles in recent years, we are currently only including data from the GOMOS and SCIAMACHY instruments onboard the ENVISAT satellite. Both provide ozone profiles from late 2002 until now. For GOMOS, we use the stellar occultation ozone profiles (version 5.0) processed by ESA (http://eopi.esa.int/registration). For SCIAMACHY, the limb ozone profiles (version 2.0) derived by the University of Bremen were used (http://www.iup.physik.uni-bremen.de/scia-arc/).

As mentioned, HALOE and most lidars also provide temperature profiles, but this is not the case for most other satellite instruments. Additional temperature profiles, therefore, were obtained from operational meteorological analyses by the US National Center for Environmental Prediction (NCEP, data for NDACC stations available at http://www. ndacc.org), and from the European Center for Medium-range Weather Forecast (ECWMF) 40-year reanalysis project (ERA-40, data available at http://data.ecmwf.int/data). Note that SAGE and GOMOS data also provide coincident temperature profiles from operational analyses by NCEP and ECWMF, respectively.

A very important source of temperature data are the infrared radiometer measurements from the sequence of Stratospheric Sounding Units (SSUs), flown from late 1978 to 2005 onboard the NOAA satellites. Here we use the SSU temperature time series compiled by Randel et al. (2009, available at http://www.sparc.sunysb.edu/html/updated_temp.html). These data have been corrected for the long-term increase in atmospheric CO_2. The most relevant SSU channel for the upper stratosphere is channel 27, which represents a vertical temperature average, with weighting function peaking near 42 km (2 hPa) and a width of ≈20 km. Fig. 2 shows the temperature record from SSU channel 27 and the synthetic channel 36x, covering a similar altitude range. For comparison rocketsonde data and model simulations are plotted as well.

Monthly mean data from all these sources were converted to ozone and temperature anomalies, and averaged over the 35 to 45 km altitude region. Anomalies were obtained by subtracting the 1998 to 2008 long-term monthly mean (annual cycle) for each calendar month (January, February, … December) from the individual monthly means starting in January 1979 and ending in April 2009. This was done separately for all individual data sources. This subtraction of the long-term annual cycle removes most systematic differences between the various instruments.

1998 to 2008 was chosen as the reference period, because a.) all instruments provided data during at least half of this period, and b.) ozone and temperature were fairly level over most of this period. An addi-

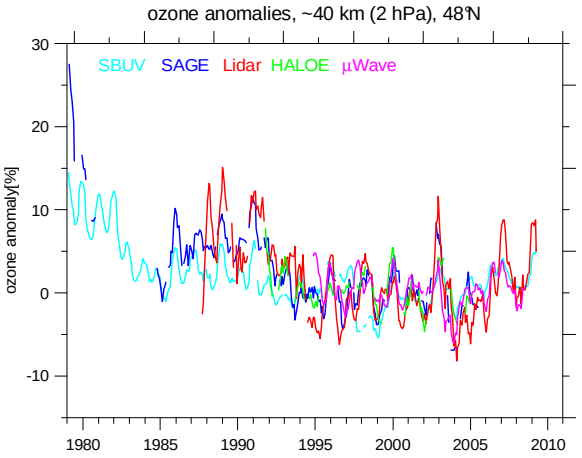

Fig. 3. Ozone anomalies measured by different instruments for the latitude of Hohenpeissenberg (48°N). Anomalies are averaged over the 35 to 45 km altitude range. Lidar and microwave data are monthly means at the station, the satellite data are zonal means. For plotting, the data were smoothed by a 5-month running mean.

tional (small) adjustment was applied to the ERA-40 temperatures (which end in 2002) so that they matched the NCEP temperatures.

3. RESULTS FOR OZONE

Fig. 3 shows the upper stratospheric ozone anomaly record for SBUV, SAGE, HALOE, the lidar at Hohenpeissenberg, and the microwave radiometer at Bern. The lidar and microwave data are monthly means at the station, whereas the satellite data are zonal mean monthly means. For SAGE and HALOE all profiles within ±5° latitude of Hohenpeissenberg (48°N, 11°E) were used, for SBUV the 5° latiitude band zonal means of the SBUV-MOD V8 data set were interpolated to 48°N. In our experience, zonal mean satellite data show better agreement with the station data, than average "overpass" data, because, especially for the solar occultation instruments, overpasses close to a station can become quite rare, e.g. less than 20 overpasses of HALOE within ±7.5° latitude and ±15° longitude of Hohenpeissenberg for the month of August over the entire 1992 to 2005 time period.

The different instrumental records in Fig. 3 show generally good agreement within 5% or better. The largest systematic differences, up to 5%, can be seen before 1993 between SBUV and SAGE. A good part of this difference comes from SBUV's ozone partial pressure versus pressure altitude coordinate system. Due to cooling of the stratosphere, this coordinate system has a long-term drift against the number density versus altitude coordinate system of the other measurements (Rosenfield et al., 2005). Additional errors are introduced by the uncertain calibration level of the individual SBUV instruments, and by the uncertain height registration of SAGE I before 1982.

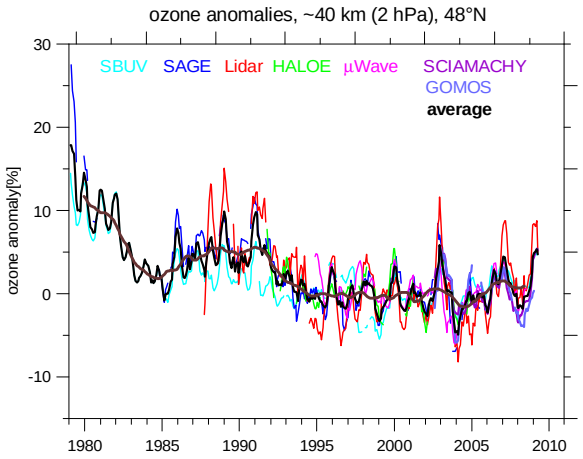

Fig. 4. Same as Fig. 3, but also showing the anomalies measured by GOMOS and SCIAMACHY, as well as the average anomaly from all available instruments. The brown line is a 25 month running mean of the average anomaly.

Overall, however, the agreement between different instruments, and their long-term accuracy appear to be quite good, better than 2%. Many of the larger differences, e.g. the larger variations seen by the lidar, appear only for a short time. Here the very different sampling of the various instruments, nearly continuous for the microwave radiometers, only at sunrise and sunset locations along the orbit for SAGE and HALOE, and only on clear nights for the lidar, play a major role.

Figure 4 shows the same data as Fig. 3, but now ozone anomalies measured by GOMOS and SCIAMACHY have been added as well. Starting in 2002 these data complement the SAGE and HALOE data which ended in 2005. GOMOS and SCIAMACHY measure ozone anomalies that are in good agreement with SBUV, the lidar and the microwave radiometer. In addition, Fig. 4 contains the average anomaly obtained by averaging over all available instruments, as well as a 26 month running mean smoothed version of this average.

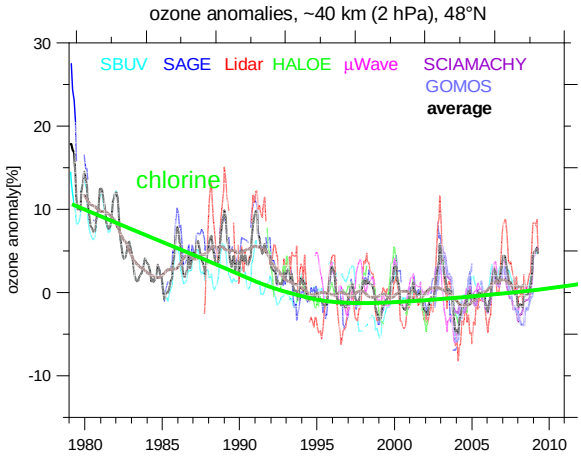

Fig. 5. Same as Fig. 4, but also showing the long term variation of ozone destruction by atmospheric chlorine. For this we simply plotted the inverted chlorine loading.

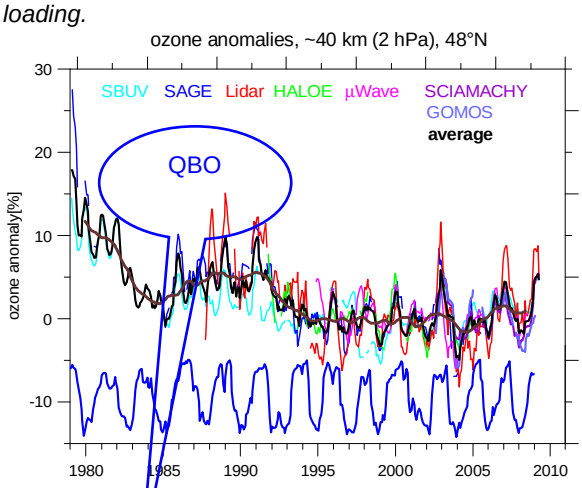

Fig. 6. Same as Fig. 4, but comparing ozone variations with (inverted) zonal wind at 10 hPa at the equator as a proxy for the QBO.

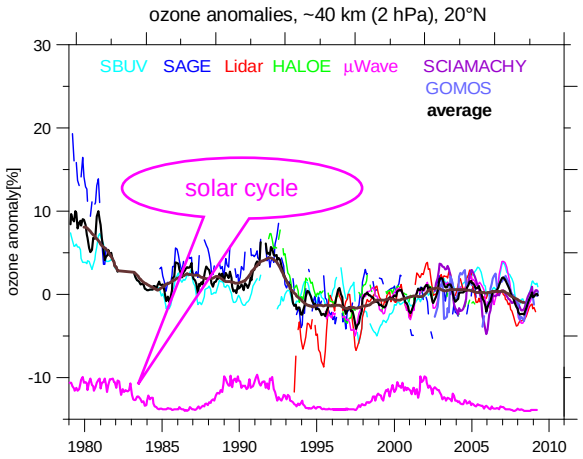

Fig. 7. Like Fig. 6, but comparing ozone variations at Hawaii with the 11-year solar cycle, as given by 10.7 cm solar radio flux.

The main long-term variations present in the upper stratospheric ozone anomalies are shown in Figs. 5 to 7. Clearly ozone follows the (inverted) long-term variation of stratospheric chlorine, with a decrease by ≈12% from 1979 to 1997, followed by a leveling and slight increase in the last 10 years (Fig. 5). A large interannual variation by up to ±5% is related to the QBO (Fig. 6). Usually higher ozone is observed in the upper stratosphere during easterly phases of the QBO (at 10 hPa), and particularly in winter. Finally, for the station at Mauna Loa, Fig. 7 shows a small variation of ozone with the 11-year solar cycle. During solar maxima, upper stratospheric ozone is a few percent higher than during solar minima. An accurate estimation of the solar cycle variation is complicated by the super-imposed effect of chlorine turning around in the 2003 solar maximum, and by the few available data sources at the time of the 1980 solar maximum.

Overall, Figure 5 shows clear signs of a beginning recovery of upper stratospheric ozone. Superimposed are substantial interannual variations, in particular due to the QBO. To be suited for the analysis of long-term variations, any time series must cover at least several QBO cycles, and preferably also at least one solar cycle. Even the SCIAMACHY and GOMOS time series that are now reaching 7 years are not long enough for this yet. To assure the comparability of different satellite time series, long and consistent time series from the ground-based instruments are very helpful.

4. RESULTS FOR TEMPERATURE

As indicated in Fig. 2, the long-term evolution of temperature should differ from that of ozone. Whereas ozone shows a clear turnaround after the year 2000, following the beginning decrease of the atmospheric chlorine loading (compare Fig. 5), temperature should show a continuing long term decline, according to Fig. 2.

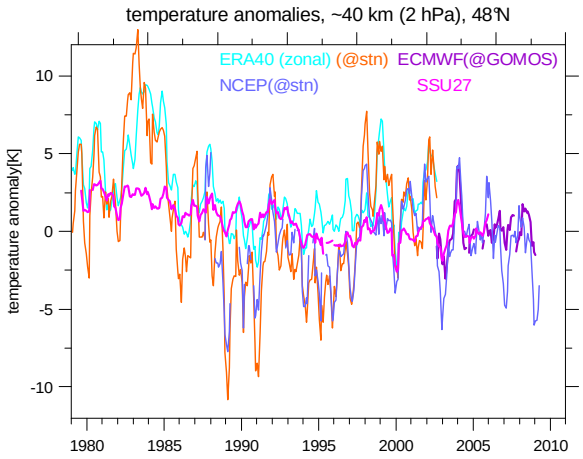

Fig. 8. Temperature anomalies for Hohenpeissenberg (48°N, 11°N) from different data sets. For ERA- 40, zonal means and station means are shown. The ECMWF operational data are zonal means at the location of the GOMOS observations. The SSU data are means over a wide zonal band, and a wide altitude range. The NCEP data are means at the station location.

Fig. 8 shows the evolution of temperature at northern mid-latitudes as reported by ERA-40 zonal means and ERA-40 local means for the Hohenpeissenberg station, as well as NCEP operational analysis at the location of the station. The first thing to note in Fig. 8 are the substantial differences between ERA40 zonal means (light blue) and ERA40 station means (orange) during the entire 1990 to 1998 period. It appears that temperature anomalies are much less zonally symmetric than ozone anomalies. The NCEP station anomalies (blue) very closely follow the ERA40 station anomalies. They are also in good

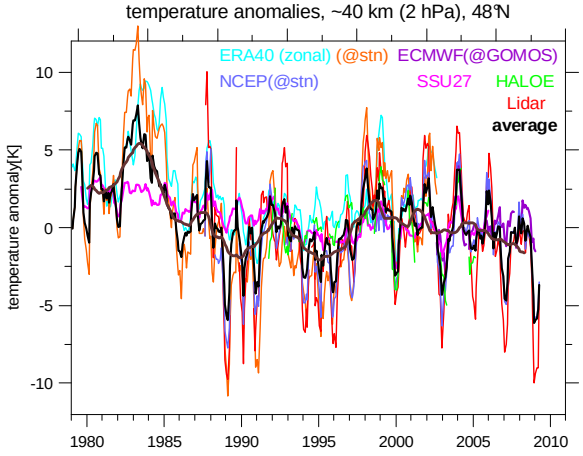

Fig. 9. Same as Fig. 8, but also showing zonal mean temperature anomalies measured by HALOE, and station mean anomalies measured by the lidar. In addition the average of all available data is shown (black line), together with 25 month running mean of the average (brown line).

agreement with the ECWMF operational analyses after 2002 (purple).

Substantial differences can be seen between the SSU zonal means (pink) and the operational analyses. At this point it is not clear whether this is due to the poor horizontal and vertical resolution of the SSU data (> 10° latitude, > 20 km altitude), or caused by inhomgeneities in the analysis systems.

In addition to the temperature anomalies shown of Fig. 8, Fig. 9 also shows the measured temperature anomalies from HALOE (zonal means) and from the Hohenpeissenberg lidar (station means). The lidar data track the NCEP and ERA40 station means quite well, although they show even larger interannual variations. The HALOE zonal means are also in good agreement with the other data sources.

The temperature variations in Figs. 8 and 9 are much more noisy than the ozone variations in the previous Figures. Differences between station means and zonal means are larger. Except for the SSU data, there is no clear indication for a temperature long-term trend. Since about 1990, temperature seems to fluctuate around a more or less constant level.

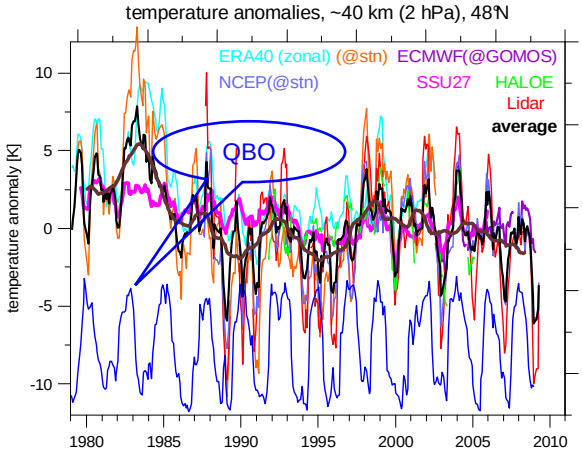

Fig. 10. Same as Fig. 9, but comparing temperature variations with zonal wind at 10 hPa at the equator as a proxy for the QBO.

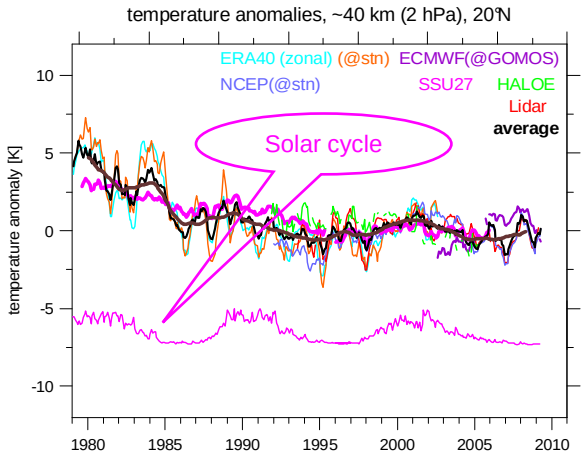

Fig. 11. Like Fig. 9, but comparing temperature variations at Hawaii with the 11-year solar cycle, as given by 10.7 cm solar radio flux.

As with ozone, the temperature variations carry a clear signature from QBO and solar cycle. Figures 10 and 11 show that QBO related temperature variations can exceed ±5 K, whereas the solar cycle variation is only around 1 K.

5. SUMMARY AND CONCLUSIONS

The long-term evolution of ozone and temperature in the 40 km region at all five stations is summarized in Figs. 12 and 13. In both Figures, results from 3-D model simulations under the Chemistry Climate Model Validation Initiative (CCMVal, Eyring et al., 2006) have been underlaid as a grey area. This grey range gives a good representation of the average and range of the model simulations. It is centered on the monthly zonal mean anomalies averaged over all models. The vertical extent corresponds to plus and minus 2 standard deviations of all model monthly means in a sliding 2 year window.

For ozone, all stations show a very similar picture. The long-term decline of ozone over the 1979 to 1997 period, due to increasing anthropogenic chlorine, is followed by a leveling and even slight increase over the last 10 years. The range of model predictions is consistent with these observed ozone variations. From Fig 12 it is clear, that ozone is following the evolution expected from the atmospheric chlorine burden (pink ESC line or grey model predictions). The Montreal protocol has successfully curbed chlorine levels. Upper stratospheric ozone is now clearly beginning to recover.

For temperature (Fig. 13), the picture is much less clear. Interannual variations are much larger than a possible long-term trend. As can be seen from the substantial differences between zonal means and station means, especially at the northern stations, longitudinal variations play a bigger role for temperature than for ozone. Consistency between different data sets is also not as good as for ozone. The SSU data show a much smoother behavior than the other data sets.

At most stations in Fig. 13, there is no clear indication for a long-term temperature trend. Rather, it seems that temperatures have been fluctuating around a more or less constant level since the 1990s. Especially at the three northerly stations, the observed variations are larger and often lie outside of the range of the CCMVal model predictions. Better agreement is found for Hawaii (20°N) and Lauder (45°S). There the range of model predictions is mor e consistent with the observed temperature anomalies, and the observations are more consistent with a long-term temperature decline.

Clearly, further work is required to obtain a good data basis for the long-term evolution of temperature. It is necessary to extend the SSU record, which has ended in 2005. Newer satellite instruments, e.g. the SABER instrument on TIMED are good candidates. Hopefully the ground station data can help to insure a homegeneous transition. Future analyses should

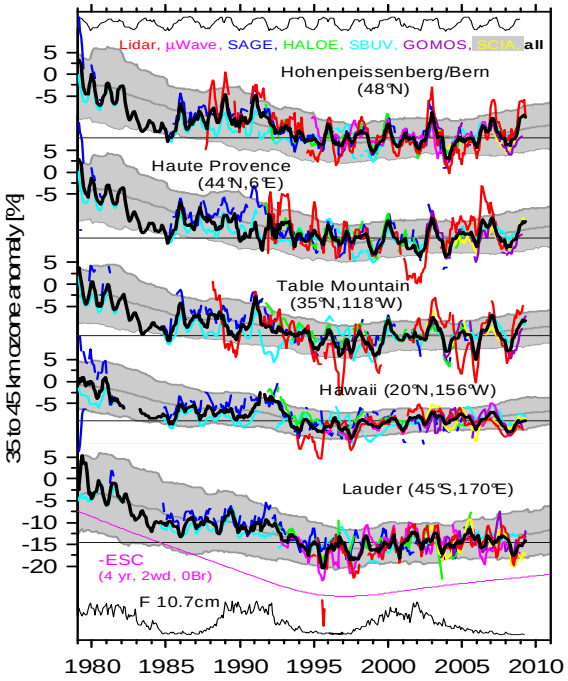

Fig. 12. Ozone anomalies observed by the different instruments at the five selected NDACC stations. The grey underlay shows the range of corresponding CCMVal simulations (see text for details).

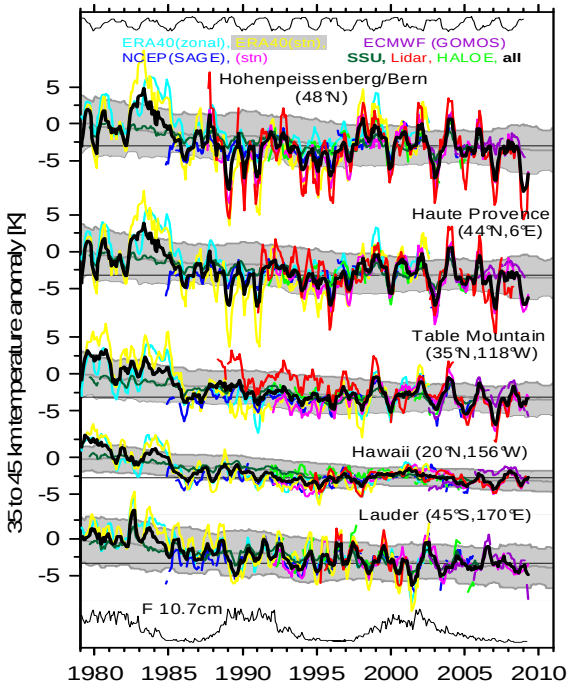

Fig. 13. Same as Fig. 12, but for temperature anomalies.

probably exclude the very variable winter data of the northerly stations.

For ozone, however, the combination of the various instruments seems to provide a stable observation system with adequate coverage. To follow the expected ozone recovery, observations need to be continued. If temperatures do decline significantly, it is even expected that ozone should return to levels higher than observed in the 1980s, because when chorine is gone, lower temperature will slow that natural ozone destruction cycle.

6. REFERENCES

Dunkerton, T., D. Delisi, and M. Baldwin, 1998: Middle Atmosphere Cooling Trend in Historical Rocketsonde Data, *Geophys. Res. Lett.*, 25(17), 3371-3374.

Eyring, V., et al., 2006: Assessment of temperature, trace species, and ozone in chemistry climate model simulations of the recent past. *J. Geophys. Res.*, 111, D22308, doi:10.1029/2006JD007327.

Newchurch, M.J., et al., 2003: Evidence for slowdown in stratospheric ozone loss: First stage of ozone recovery. *J. Geophys. Res.*, 108, 4507, doi:10.1029/2003JD003471.

Ramaswamy, V., et al., 2001, Stratospheric temperature trends: observations and model simulations, *Rev. Geophys,*, 39, pp. 71-122.

Randel W.J., et al., 2009: An update of observed stratospheric temperature trends, *J. Geophys. Res.*, 114, D02107, doi:10.1029/2008JD010421.

Rosenfield, J.E., Frith, S.M. and Stolarski, R.S., 2005, Version 8 SBUV ozone profile trends compared with trends from a zonally averaged chemical model, *Geophys. Res. Lett.*, 110, D12302, doi: 10.1029/2004JD005466.

Steinbrecht W., et al., 2006: Long-term evolution of upper stratospheric ozone at selected stations of the Network for the Detection of Stratospheric Change (NDSC). *J. Geophys. Res.*, 111, D10308, doi:10.1029/2005JD006454.

WMO (World Meteorological Organization), United Nations Environment Programme, 2007, Scientific Assessment of Ozone Depletion: 2006. Global Ozone Research and Monitoring Project-Report No. 50 (Geneva, Switzerland: WMO/ UNEP).